

International Journal of Modern Physics A
World Scientific Publishing Company

NEW PHYSICS EFFECTS IN THE FLAVOR-CHANGING
NEUTRAL COUPLINGS OF THE TOP QUARK

F. LARIOS

Departamento de Física Aplicada, CINVESTAV-Mérida, A.P. 73,
97310 Mérida, Yuc., México
larios@mda.cinvestav.mx

R. MARTINEZ

Departamento de Física, Universidad Nacional, Apartado aéreo 14490,
Bogotá, Colombia
remartinez@unaledu.co

M. A. PEREZ

Departamento de Física, Cinvestav, A.P. 14-740, 07000,
México D.F., México
mperez@s.cinvestav.mx

Received Day Month Year

Revised Day Month Year

We survey the flavor-changing neutral couplings (FCNC) of the top quark predicted by some extensions of the Standard Model: THDM, SUSY, L-R symmetric, TC2, 331, and models with extra quarks. Since the expected sensitivity of the LHC and ILC for the ttV ($V = \gamma, Z$) and ttH couplings is of order of a few percent, we emphasize the importance of any new physics effect that gives a prediction for these FCNC couplings within this limit. We also review the constraints imposed on these couplings from low-energy precision measurements.

Keywords: top quark, new physics, flavor-changing neutral decays.

PACS numbers: 14.65.Ha, 12.15.Mm, 12.60.-i, 12.60.Cn

1. Introduction

The weak neutral current (WNC) was the primary prediction to be tested in the electroweak $SU(2) \times U(1)$ standard model (SM). The flavor-conserving structure of the WNC has been verified with high precision in many processes¹. In the SM, there are no flavor changing neutral couplings (FCNC) mediated by the Z , γ , g gauge bosons nor the Higgs boson H at tree level because the fermions are rotated from gauge to mass eigenstates by unitary diagonalization matrices². Furthermore, the top-quark FCNC induced by radiative effects are also highly suppressed^{3;4;5}: the higher order contributions induced by the charged currents are proportional to

2 F. Larios, R. Martinez and M. A. Perez

$(m_i^2 - m_j^2)/M_W^2$, where $m_{i,j}$ are the masses of the quarks circulating in the loop and M_W is the W gauge boson mass. As a consequence, in the SM all top-quark FCNC transitions $t \rightarrow qV; qH$, with $V = Z; \gamma; g$, which involve down-type quarks in the loops, are suppressed far below the observable level at existing or upcoming high energy colliders^{3;4;5}. For example, in the $t \rightarrow cV$ transitions the scale of the respective partial widths is set by the b quark mass^{3;4},

$$\Gamma(t \rightarrow V_i c) = |Y_{bc}^i|^2 \frac{m_b}{m_t} \left(\frac{m_b}{M_W}\right)^4 \left(1 - \frac{m_{V_i}^2}{m_t^2}\right) \quad (1)$$

where Y_i is the respective coupling for each gauge boson V_i . From the above result, it follows the approximated branching ratios $\text{BR}(t \rightarrow cZ) \sim 10^{-13}$ and $\text{BR}(t \rightarrow c\gamma) \sim 10^{-11}$. In contrast, in the $b \rightarrow s$ transitions the leading contribution is proportional to m_t^4/M_W^4 and thus the GIM mechanism² induces in this case an enhancement factor. In a similar way, it has been realized that some top-quark FCNC decay modes can be enhanced by several orders of magnitude in scenarios beyond the SM, and some of them falling within the LHC's reach. In this case, the enhancement arises either from a large virtual mass or from the couplings involved in the loop. Top-quark FCNC processes may thus serve as a window for probing effects induced by new physics.

The absence of the vertex Htc at tree-level in the SM can be traced down to the presence of only one Higgs doublet. The process involved in the diagonalization of the fermion masses induces simultaneously diagonal Yukawa couplings for the physical Higgs boson. In models with more than one Higgs doublet, additional conditions have to be imposed to ensure that no FCNC arise at tree level. In particular, a discrete symmetry that makes quarks of same charge to interact with only one of the two (or more) Higgs doublets will, by the Glashow–Weinberg mechanism, cause all the Yukawa couplings involving physical neutral Higgs boson states become diagonal⁶. On the other hand, without any FCNC suppression mechanism these type of models may produce tqH couplings at tree level, which in turn may induce large enhancements of the FCNC tqV by radiative effects⁷. The interest in FCNC top-quark physics is expected to increase since processes involving top and Higgs FCNC will be examined with significant precision at both the LHC and ILC. In the first case, with a LHC luminosity of 100 fb^{-1} , 80 million of tt pairs per year will make it possible to reach the following limits⁸:

$$\begin{aligned} \text{BR}(t \rightarrow cH) &< 6 \cdot 10^{-5}; \\ \text{BR}(t \rightarrow c) &< 1 \cdot 10^{-5}; \\ \text{BR}(t \rightarrow cZ) &< 4 \cdot 10^{-5}; \\ \text{BR}(t \rightarrow c\gamma) &< 2 \cdot 10^{-5}; \end{aligned} \quad (2)$$

while at the ILC, with an integrated luminosity of $100 - 200 \text{ fb}^{-1}$ one can hope to

reach the sensibilities^{8,9}:

$$\begin{aligned} \text{BR}(t \rightarrow cH) &< 4.5 \cdot 10^{-5} \\ \text{BR}(t \rightarrow c\gamma) &< 7.7 \cdot 10^{-6} \end{aligned} \quad (3)$$

The goal of the present review is to bring together much of what is currently known on top-quark FCNC. We will concentrate on the predictions made by different extensions of the SM as well as the constraints imposed on these couplings from low-energy precision measurements. The physics associated to the production mechanisms of the processes induced by the top-quark FCNC at future accelerators have been surveyed in several reviews¹⁰ and will not be considered here. Our interest is to compare the predictions on the top-quark FCNC made by the following models: SUSY, two-Higgs doublets models (THDM), top-color assisted Technicolor, left-right symmetric models, 331 models, and models with extra quark singlets or extra sequential quarks. We will introduce first the SM predictions, and then we will address each one of these models in the following sections. The last section will be devoted to the analysis of the model-independent constraints for these couplings.

2. Top-quark SM couplings

Although the top quark was discovered ten years ago^{11,12}, its couplings to the gauge bosons $g;W$ and Z have not been yet measured directly¹⁰. Current data provide only weak indirect limits on the ttW and ttV couplings, with $V = g;Z$. We will use the following parameterization corresponding to effective ttV interactions with quarks on-shell and the gauge bosons coupled effectively to massless fermions¹³:

$$\begin{aligned} \Gamma_{ttV}^{\mu}(k^2; q; q) = & ief \left(F_{1V}^V(k^2) + \frac{1}{5} F_{1A}^V(k^2) \right) + \frac{1}{2m_t} (q + \not{q}) \left(iF_{2V}^V(k^2) \right. \\ & \left. + \frac{1}{5} F_{2A}^V(k^2) \right) g \end{aligned} \quad (4)$$

where m_t is the top quark mass, $q(q)$ is the outgoing top (anti-top) quark momentum, $k^2 = (q + q)^2$, and at tree level in the SM,

$$\begin{aligned} F_{1V}^{iSM} &= \frac{2}{3} e; & F_{1A}^{iSM} &= 0; \\ F_{1V}^{ZiSM} &= \frac{e}{4s_w c_w} \left(1 - \frac{8}{3} s_w^2 \right); & F_{1A}^{ZiSM} &= \frac{e}{4s_w c_w}; \\ F_{2V}^{iSM} &= F_{2V}^{ZiSM} = 0; & F_{2A}^{iSM} &= F_{2A}^{ZiSM} = 0; \end{aligned} \quad (5)$$

where $c_w = \cos \theta_w$, $s_w = \sin \theta_w$ and θ_w is the weak mixing angle. The functions $F_{1V}^V(0)$ and $F_{1A}^V(0)$ are the ttV vector and axial vector form factors, $F_{2V}^g(0) = 2e=3(g_t^2)=2$; $F_{2A}^g(0) = 2m_t d_t^g$, with g_t^g and d_t^g the magnetic and the (CP-violating) electric dipole form factors of the top quark. There are similar relations for $F_{2V}^Z(0)$ and $F_{2A}^Z(0)$ with the weak magnetic and electric dipole form factors of the Z gauge boson.

4 F. Larios, R. Martinez and M. A. Perez

It is possible to parameterize possible deviations from the SM predictions for the $t\bar{t}W$ and $t\bar{t}Z$ couplings in terms of only four coefficients $\kappa_{L,R}^{NC}$ and $\kappa_{L,R}^{CC}$ defined as follows¹⁴:

$$\begin{aligned} \mathcal{L} = & \frac{g}{2c_W} \left[1 + \frac{4s_W^2}{3} \kappa_L^{NC} \right] \bar{t}_L \gamma^\mu t_L Z + \frac{g}{2c_W} \left[\frac{4s_W^2}{3} + \kappa_R^{NC} \right] \bar{t}_R \gamma^\mu t_R Z \\ & + \frac{g}{2} \left[1 + \kappa_L^{CC} \right] \bar{t}_L \gamma^\mu b_L W^+ + \frac{g}{2} \left[1 + \kappa_L^{CC_Y} \right] \bar{t}_L \gamma^\mu b_L W \\ & + \frac{g}{2} \kappa_R^{CC} \bar{t}_R \gamma^\mu b_R W^+ + \frac{g}{2} \kappa_R^{CC_Y} \bar{t}_R \gamma^\mu b_R W \end{aligned} \quad (6)$$

where t_L denotes a top quark with left-handed chirality, etc. While the $t\bar{t}Z$ vector and axial-vector couplings are tightly constrained by the LEP data^{14,15}, the right handed $t\bar{t}W$ coupling is severely bounded by the observed $b \rightarrow s$ rate¹⁶ at the 2% level,

$$\begin{aligned} \text{Re}(\kappa_R^{CC}) & \leq 0.4 \cdot 10^{-2} \\ 0.0035 & \leq \text{Re}(\kappa_R^{CC}) + 20 \text{Im}(\kappa_R^{CC}) \leq 0.0039 \end{aligned} \quad (7)$$

On the other hand, LEP/SLC data also constrains the other top-quark couplings included in Eq.(4). Even though these data do not restrict all the anomalous terms, they induce the following inequalities

$$\begin{aligned} 0.019 & \leq \left(\kappa_R^{NC} - \kappa_L^{NC} \right) \left(\kappa_R^{NC} - \kappa_L^{NC} \right)^2 + \kappa_L^{CC} + \kappa_L^{CC}{}^2 \leq 0.0013 \\ 0.33 & \leq \left(\kappa_R^{NC} - 4 \kappa_L^{NC} \right) \left(1 + 2 \kappa_L^{CC} \right) \leq 0.1 \\ \kappa_L^{CC} & \leq \kappa_L^{NC} \leq \kappa_R^{NC} \end{aligned} \quad (8)$$

These relations impose in turn strong correlations on the couplings so that if only one coupling, κ_L^{CC} for instance, is not zero, the others are forced to be about the same order of magnitude¹⁶.

On the other hand, at an e^+e^- linear collider (ILC) with $\sqrt{s} = 500 \text{ GeV}$, and an integrated luminosity of $100 - 200 \text{ fb}^{-1}$, it will be possible to measure the $t\bar{t}V$ couplings in $t\bar{t}$ production with a few percent precision⁹. In the LHC, with an integrated luminosity of 30 fb^{-1} , it will be possible to probe the $t\bar{t}$ coupling with a precision of $10 - 35\%$ per experiment¹⁷. The sensitivity limits on the $t\bar{t}Z$ couplings will be significantly weaker than those expected for the $t\bar{t}$ couplings. Thus, the ILC will be the best place to probe the $t\bar{t}Z$ couplings at the few percent level.

The most general effective Lagrangian describing the FCNC top-quark interactions with a light quark $q^0 = u, c$, containing terms up to dimension five, can be

written as¹⁸

$$\begin{aligned}
 L = & \text{tf} \frac{ie}{2m_t} (tq^0 + i\tilde{t}q^0) F \\
 & + \text{tf} \frac{ig_s}{2m_t} (tq^0g + i\tilde{t}q^0g) \frac{a}{2} G_a \\
 & + \frac{i}{2m_t} (tq^0Z + i\tilde{t}q^0Z) Z \\
 & + \frac{g}{2C_W} (v_{tq^0Z} + a_{tq^0Z}) Z \\
 & + \frac{g}{2} (h_{tq^0H} + i\tilde{h}_{tq^0H}) H gq^0,
 \end{aligned} \tag{9}$$

where we have assumed also that the top quark and the neutral bosons are on shell or coupled effectively to massless fermions. In terms of these coupling constants, the respective partial widths for FCNC decays are given by⁸

$$\begin{aligned}
 \Gamma(t \rightarrow qZ) &= \frac{j_{tqZ}^2 + j_{\tilde{t}qZ}^2}{32s_W^2 c_W^2} \frac{m_t^3}{M_Z^2} \left(1 + \frac{M_Z^2}{m_t^2} \right) \left(1 + 2 \frac{M_Z^2}{m_t^2} \right) \\
 \Gamma(t \rightarrow qZ) &= \frac{j_{VtqZ}^2 + j_{AtqZ}^2}{16s_W^2 c_W^2} \frac{m_t^3}{M_Z^2} \left(2 + \frac{M_Z^2}{m_t^2} \right) \\
 \Gamma(t \rightarrow q) &= \frac{j_{tq}^2 + j_{\tilde{t}q}^2}{2} m_t \\
 \Gamma(t \rightarrow qg) &= \frac{2}{3} j_{tqg}^2 m_t \\
 \Gamma(t \rightarrow qH) &= \frac{j_{htqH}^2 + j_{\tilde{h}tqH}^2}{32s_W^2} \frac{m_t^3}{M_H^2} \tag{10}
 \end{aligned}$$

If we use $m_t = 178.0 \pm 4.3$ GeV, $(m_b) = 1 \pm 128.921$, $s_W^2 = 0.2342$, $c_W^2 = 0.7658$, $m_H = 115$ GeV and the tree level prediction for the leading $t \rightarrow bW$ decay¹

$$\Gamma(t \rightarrow bW) = \frac{j_{Vtb}^2}{16s_W^2} \frac{m_t^3}{M_W^2} \left(1 + 3 \frac{M_W^2}{m_t^2} + 2 \frac{M_W^4}{m_t^4} \right); \tag{11}$$

an update of the original SM calculations^{3,4,5} for the FCNC top-quark branching ratios gives thus the following results⁸

$$\begin{aligned}
 BR(t \rightarrow cq) &= (4.6^{+1.2}_{-1.0} \text{ } 0.2 \text{ } 0.4^{+1.6}_{-0.5}) \cdot 10^{-14} \\
 BR(t \rightarrow qg) &= (4.6^{+1.1}_{-0.9} \text{ } 0.2 \text{ } 0.4^{+2.1}_{-0.7}) \cdot 10^{-12} \\
 BR(t \rightarrow qZ) &= 1 \cdot 10^{-14} \\
 BR(t \rightarrow qH) &= 3 \cdot 10^{-15}
 \end{aligned} \tag{12}$$

where the uncertainties shown in the $t \rightarrow cq$ branching ratios are associated to the top and bottom quark masses, the CKM matrix elements and the renormalization scale. These updated results are about one order of magnitude smaller than the ones previously obtained^{3,4,5}. For the decays involving the u quark, the respective BR are a factor $|j_{ub}|^2 = |j_{cb}|^2 = 0.0079$ smaller than those shown in (12).

6 F. Larios, R. Martínez and M. A. Pérez

3. Two Higgs doublet models

One of the simplest extensions of the SM adds a new complex $SU(2) \times U(1)$ scalar doublet to the Higgs sector and it is known as the Two Higgs Doublet Model (THDM) ⁶. There are three possible versions of this model depending on how the two doublets couple to the fermion sector. In particular, models I and II (THDM -I, THDM -II) include natural flavor conservation ^{6;19}, while model III (THDM -III) has the simplest extended Higgs sector that naturally introduces FCNC at the tree level ^{20;21;22}. The most general THDM scalar potential, which is invariant under both $SU(2) \times U(1)$ and CP symmetries, is given by ¹⁹

$$V(\phi_1; \phi_2) = \lambda_1 (\phi_1^\dagger \phi_1 - v_1^2)^2 + \lambda_2 (\phi_2^\dagger \phi_2 - v_2^2)^2 + \lambda_3 ((\phi_1^\dagger \phi_1) + (\phi_2^\dagger \phi_2))^2 + \lambda_4 (\phi_1^\dagger \phi_2 + \phi_2^\dagger \phi_1) + \lambda_5 \text{Re}(\phi_1^\dagger \phi_2) + \lambda_6 \text{Im}(\phi_1^\dagger \phi_2) \quad (13)$$

where ϕ_1 and ϕ_2 are the two Higgs doublets with weak hypercharge $Y=1$, v_1 and v_2 are their respective vacuum expectation values, and the six parameters are real. The dimension-two term $\lambda_5 \text{Re}(\phi_1^\dagger \phi_2)$ violates softly the discrete symmetry $\phi_i \rightarrow -\phi_i$; which is essential to induce natural flavor conservation in models I and II ⁶.

After the electroweak symmetry breakdown, three of the original eight degrees of freedom associated to ϕ_1 and ϕ_2 correspond to the three Goldstone bosons ($G^\pm; G^0$), while the other five degrees of freedom reduce to five physical Higgs bosons: h, H (both CP-even), A (CP-odd), and H^\pm . The combination $v^2 = v_1^2 + v_2^2$ is fixed by the electroweak scale $v = (\sqrt{2}G_F)^{-1/2}$ and there are still 7 independent parameters, which are given in terms of four physical scalar masses ($m_h; m_H; m_A; m_{H^\pm}$), two mixing angles ($\tan\beta = v_2/v_1$ and α) and the soft breaking term λ_5 .

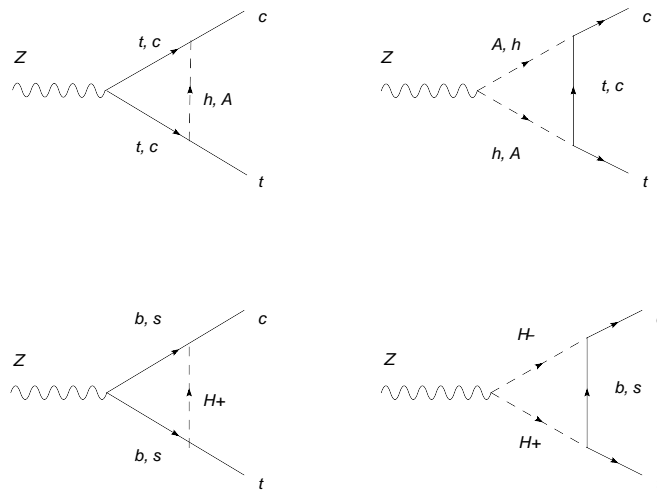


Fig. 1. Generic contribution to the tcZ and ct vertices in the THDM -III.

The three versions of the THDM are distinguished by their Yukawa couplings,

$$L^{\text{THDM}} = \sum_{ij} \overline{Q}_{iL}^U e_1 U_{jR} + \sum_{ij} \overline{Q}_{iL}^D d_1 D_{jR} + \sum_{ij} \overline{Q}_{iL}^U e_2 U_{jR} + \sum_{ij} \overline{Q}_{iL}^D d_2 D_{jR} + \text{h.c.} \quad (14)$$

where $\overline{Q}_{ij}^U = 0$ for model I and $\overline{Q}_{ij}^D = 0$ for model II. For model III all \overline{Q}_{ij}^U 's and \overline{Q}_{ij}^D 's are different from zero. While models I and II do not generate FCNC at tree level, due to the Glashow–Weinberg theorem⁶, in model III the following FCNC interaction is obtained after the spontaneous symmetry breaking $\langle \phi_1 \rangle = (0; v = \sqrt{2})$, $\langle \phi_2 \rangle = 0$,

$$L^{\text{THDM}} = \sum_{ij} \sin \theta_{ij} f_i f_j h + \sum_{ij} \cos \theta_{ij} f_i f_j H + \sum_{ij} \cos \theta_{ij} f_i f_j A + \text{h.c.} \quad (15)$$

In THDM –I and THDM –II the FCNC decay modes $t \rightarrow c \nu$ are dominated by the one-loop diagrams with a virtual H and their respective branching ratios are only sensitive to m_H and $\tan \beta$. The largest enhancements are found for THDM –II with $120 \text{ GeV} < m_H < 250 \text{ GeV}$ and $\tan \beta > 10$: $\text{BR}(t \rightarrow c \nu) \sim 10^{-7} - 10^{-10}$, $\text{BR}(t \rightarrow c \eta) \sim 10^{-5} - 10^{-9}$; $\text{BR}(t \rightarrow c Z) \sim 10^{-8} - 10^{-11}$ ^{4;23}.

In the case of the FCNC decay mode with a light Higgs scalar $t \rightarrow ch$, the enhancement is spectacular $\text{BR}(t \rightarrow ch) \sim 8 \times 10^{-5}$ for large $\tan \beta$ and a light charged Higgs mass. This time the pure scalar couplings hH^+H and hG^+H play a crucial role²⁴.

On the other hand, in the THDM –III the heavy neutral scalar and pseudoscalar Higgs bosons H and A have non-diagonal couplings to fermions at the tree level. The FCNC decay modes $t \rightarrow c \nu$ and $t \rightarrow ch$ proceed at the one-loop level due to the exchange of H ; A and H (Fig. 1). The respective branching ratios may be enhanced by several orders of magnitude, for reasonable values of the THDM –III parameters, with respect to the SM predictions: $\text{BR}(t \rightarrow c \eta) \sim 10^{-4} - 10^{-8}$; $\text{BR}(t \rightarrow c \nu) \sim 10^{-7} - 10^{-11}$; $\text{BR}(t \rightarrow c Z) \sim 10^{-6} - 10^{-8}$ ^{22;25;26}.

4. Supersymmetric models

Theories with low-energy SUSY have emerged as the most attractive candidates for physics beyond the SM²⁷. In particular, they provide an elegant resolution of the hierarchy problem: SUSY relates the scalar and fermionic sectors. Thus, the chiral symmetries which protect the masses of the fermions also protect the scalar masses from quadratic divergences. In the unbroken SUSY world, each known particle has a superpartner that differs in spin by 1/2 and is related to the original particle by a SUSY transformation. However, SUSY must be a broken symmetry. Otherwise, the masses of all new superpartners would be equal to the known particle spectrum. Therefore, the effective Lagrangian at the electroweak scale is expected to be parameterized by a general set of SUSY-breaking terms if the attractive features of SUSY are to be a part of the physics beyond the SM. This version of SUSY is known as the minimal Supersymmetric standard model (MSSM).

8 F. Larios, R. Martinez and M. A. Perez

The source of flavor violation in the MSSM arises from the possible misalignment between the rotations that diagonalize the quark and squark sectors. The superpotential of the MSSM Lagrangian is given by

$$W = \sum_{ij} L_i^L E_j^c H_1 + \sum_{ij} H_1 Q_i D_j^c + \sum_{ij} U_i^c Q_j H_2 + H_1 H_2 \quad (16)$$

where L_i and Q_i , $i = 1; 2; 3$ are the chiral superfields for the $SU(2)_L$ doublets for leptons and quarks, $E^c; D^c$ and U^c correspond to the respective $SU(2)_L$ fermion singlets. H_1 and H_2 represent two $SU(2)$ Higgs doublets with hypercharge -1 and $+1$, respectively. The MSSM with explicit R -parity violation includes the following terms in the superpotential:

$$W_R = \sum_{ijk} L_i L_j F_k^c + \sum_{ijk} L_i Q_j D_k^c + \sum_{ijk} U_i^c D_j^c D_k^c : \quad (17)$$

These terms generate a direct violation of R -parity invariance $(-1)^{3B+L+2S}$ with B and L the leptonic and baryonic quantum numbers, and S the spin of each field. The known bounds on the proton decay and the low-energy FCNC precision measurements set strong constraints on the \sum_{ijk} couplings²⁷. The soft-SUSY-breaking terms responsible for the non-minimal squark family ($\tilde{Q}; \tilde{u}; \tilde{d}$) mixing are given by

$$\begin{aligned} L_{\text{soft}} = & (m_Q^2)_{ij} \tilde{Q}^i \tilde{Q}^j + (m_D^2)_{ij} \tilde{U}^{i+} \tilde{U}^j + (m_{\tilde{D}}^2)_{ij} \tilde{D}^{i+} \tilde{D}^j \\ & + A_{ij}^U \tilde{Q}^i \tilde{U}_R^j h_2 + A_{ij}^D \tilde{Q}^i \tilde{D}_R^j h_1 : \end{aligned} \quad (18)$$

The FCNC effects come from the non-diagonal entries in the bilinear terms $M_Q^2; M_{\tilde{Q}}^2$ and $M_{\tilde{D}}^2$, as well as from the trilinear terms A^U and A^D . If this model becomes universal in the three families at the GUT scale, then we have

$$m_Q^2 = m_{\tilde{U}}^2 = m_{\tilde{D}}^2 = m_\circ^2$$

and

$$A_{ij}^{U,D} = A_\circ \delta_{ij}^{U,D} : \quad (19)$$

As far as the top-quark FCNC are concerned, the decays $t \rightarrow cV$ have been studied extensively in the MSSM. The first studies²⁸ considered one-loop SUSY-QCD and SUSY-EW contributions, which were later generalized in order to include the left-handed (LH) and right-handed (RH) squark mixings²⁹. The SUSY-EW corrections were further generalized and included the neutralino- $q\bar{q}$ loop³⁰, as well as the relevant SUSY mixing angles and diagrams involving a helicity flip in the gluino line^{31;32}. While the first calculations obtained $BR(t \rightarrow cV)$ of the order of $10^{-6} - 10^{-8}$, every new study improved these results until the range of values $BR(t \rightarrow c\gamma) \sim 10^{-5}$, $BR(t \rightarrow cZ) \sim 10^{-6}$, $BR(t \rightarrow cV) \sim 10^{-6}$ were reached. However, they are still below the estimated sensitivity at the LHC with an integrated luminosity of 100 fb^{-1} (see Eq. 2). Similar results were obtained in a MSSM with a light right-handed top-squark and a large mixing between the first or second and the third generation of up-squarks³³.

Recently, the FCNC top-quark decays have been re-analyzed in the so-called unconstrained MSSM³⁴, where the assumptions on the soft breaking terms are relaxed and new sources of flavor violation appear in the sfermion mass matrices. In this case the neutralino- $q\bar{q}$ and gluino- $q\bar{q}$ couplings induce larger contributions to the FCNC processes: $BR(t \rightarrow c\gamma) \sim 10^{-6}$, $BR(t \rightarrow cZ) \sim 10^{-6}$, $BR(t \rightarrow c\gamma) \sim 10^{-4}$, with the last one probably measurable at the LHC³⁵. If these top-quark decays are not observed at the LHC, upper bounds will be set on specific soft SUSY breaking parameters.

Another enhancement has been reported³⁶ for the $t \rightarrow cV$ decays induced by B -violating couplings in broken R -parity MSSM: $BR(t \rightarrow c\gamma) \sim 10^{-3}$, $BR(t \rightarrow cZ) \sim 10^{-5}$, $BR(t \rightarrow cZ) \sim 10^{-4}$, which are definitely within the LHC's reach (Eq. 2).

On the other hand, while the $t \rightarrow cH$ decay is the less favored channel in the SM^{4,5}, it is this FCNC channel which shows the most dramatic enhancements due to new physics effects. In some SUSY extensions its BR can be ten orders of magnitude larger than the SM prediction. This possibility arises not only because in some models the FCNC vertex $t\bar{c}H$ can be generated at tree level, but also because the GIM suppression does not apply in some loops. In particular, the gluino-mediated FCNC couplings $u_a \bar{u}_b \tilde{g}$ induces a $BR(t \rightarrow cH) \sim 10^{-4}$, where h is the lightest CP-even Higgs boson predicted in the MSSM^{31;32;37}. The branching fraction for this channel has been also found to be as large as $10^{-3} - 10^{-5}$ in a minimal SUSY FCNC scenario in which all the observable FCNC effects come from squark mixings $e^{-\tau}$ induced by the non-diagonal scalar trilinear interactions³⁸. However, it has been pointed out recently that the electroweak precision measurements may impose constraints on this squark mixing, which in turn decrease the MSSM prediction for the FCNC top quark processes³⁹.

If R -parity violation is included in the MSSM, $t \rightarrow cH$ receives new contributions from the loops with an exchange of a single sparticle that involves the third generation of fermions. As a consequence, the mass suppression is less severe than in the purely MSSM⁴⁰. In this case the respective branching ratio can be as high as 10^{-5} in some part of the parameter space. It should be mentioned that in all these cases, the $BR(t \rightarrow cH)$ falls off quickly for heavier sparticles in the loops.

The occurrence of tree-level FCNC has also been studied in supersymmetric multi-Higgs doublet models⁴¹. As expected, it was found that the matrices which diagonalize the quark mass matrices do not, in general, diagonalize also the corresponding Yukawa couplings. As a consequence, both scalar and pseudoscalar Higgs-quark-quark interactions may exhibit a strong non-diagonality in flavor space. For example, one-loop contributions to low-energy observables require a Higgs spectrum at least of order 10 TeV in order to suppress appreciably FCNC of light quarks⁴¹.

10 F. Larios, R. Martinez and M. A. Perez

5. Topcolor-assisted Technicolor

In Technicolor theories, the electroweak symmetry breaking mechanism arises from a new, strongly coupled gauge interaction at TeV energy scales⁴². Quark and lepton mass matrices appear from the embedding of Technicolor in a larger gauge theory, extended Technicolor⁴³, which must be broken sequentially from energies of order 10^3 TeV down to the 1 TeV level. However, the simplest QCD-like extended Technicolor (ETC) model leads into problems with the LEP precision measurements data¹. The topcolor scenario was proposed in order to make the predictions consistent with the LEP data and to explain the large top quark mass. Topcolor-assisted Technicolor (TC2) models⁴⁴, flavor-universal TC2 models⁴⁵, top see-saw models⁴⁶, and the top flavor see-saw models⁴⁷ are examples of the topcolor scenario⁴⁸.

In the TC2 model, the topcolor interactions give rise to the main part of the top quark mass $(1 - \epsilon)m_t$, with the model-dependent parameter ϵ in the range $0.03 < \epsilon < 0.1$ ⁴⁴. The ETC interactions are responsible for the remaining part of the top quark mass, ϵm_t . This model predicts three heavy top-pions (π_t^0 ; π_t^\pm) and one top-Higgs boson h_t^0 with large Yukawa couplings to the third generation of fermions, which thus can induce new top quark FCNC. Early calculations, in the framework of the simplest ETC models, already produced large enhancements for the FCNC decay modes $t \rightarrow c \gamma$ ⁴⁹. In the TC2 model, there were also found⁵⁰ large enhancements for these decay modes which arose from the virtual contributions of the top-pions and the top-Higgs boson for reasonable values of the TC2 parameters: $BR(t \rightarrow c \gamma) \sim 10^{-5}$, $BR(t \rightarrow c Z) \sim 10^{-5}$, $BR(t \rightarrow c \pi) \sim 10^{-7}$.

The contribution of an extra neutral gauge boson Z^0 to the $t \rightarrow c$ decay mode has been studied also in the framework of the TC2 model and the so-called 331 model⁵¹. Even though the Z^0 boson predicted in these models couples in a non-universal way to the third generation of fermions, it was found that its contribution to the branching ratio of $t \rightarrow c$ is at most of order of 10^{-8} for $m_{Z^0} = 500$ GeV⁵².

6. Left-Right Symmetric Models

Left-Right (LR) symmetric models are based on the gauge group $SU(2)_L \times SU(2)_R \times U(1)_{B-L}$. Their general aim is to understand the origin of parity violation in low-energy weak interactions. This gauge symmetry allows a seesaw mechanism and predicts naturally neutrino masses and mixing⁵³. FCNC top-quark decays have been studied in the alternative LR symmetric model⁵⁴, which is a new formulation of these models with an enlarged fermion sector: it includes vector-like heavy fermions in order to explain the fermionic mass hierarchy. Because of the presence of extra quarks, the CKM mass matrix is not unitary and FCNC may exist at tree level. In particular, there is a top-charm mixing angle which induces the tree level couplings $t c Z$ and $t c H$. Precision measurements at LEP impose rather weak constraints on this mixing angle, which in turn allows FCNC branching ratios as high as $BR(t \rightarrow c H) \sim 10^{-4}$ ⁵⁵.

The $t \rightarrow cV$ decay modes have been analyzed in two SUSY versions of LR symmetric models: the constrained or flavor-diagonal case, in which the only source of flavor violation comes also from the CKM matrix in the quark sector, and the unconstrained model, in which soft SUSY breaking parameters are allowed to induce flavor-dependent mixings in the squark mass matrix⁵⁶. The respective branching ratios were calculated in both cases at the one-loop level with contributions arising from virtual squarks, gluinos, charginos and neutralinos. In the flavor-diagonal case, the FCNC top quark branching ratios can not exceed 10^{-5} (10^{-6}) for the gluon ($=Z$) decay mode. On the other hand, in the unconstrained LR SUSY model, where flavor-changing elements in the squark mass matrix are allowed to be arbitrarily large only for the mixing between the second and third generations, there are more favorable enhancements: $BR(t \rightarrow cg) \sim 10^{-4}$; $BR(t \rightarrow cz) \sim 10^{-5}$ and $BR(t \rightarrow cc) \sim 10^{-6}$ ⁵⁶.

7. Models with Extra Quarks

In models with extra quarks, the CKM matrix is no longer unitary and the $t\bar{c}Z$ and $t\bar{c}H$ couplings may arise at the tree level. When the new quarks are $SU(2)_L$ $Q = 2=3$ singlets, present experimental data allow large branching ratios: $BR(t \rightarrow cZ) \sim 1\text{--}10^{-4}$ and $BR(t \rightarrow cH) \sim 4\text{--}10^{-5}$ ⁸. The decay rates for $t \rightarrow cg; c$ are induced at the one-loop level but they receive only moderate enhancements: $BR(t \rightarrow cg) \sim 1\text{--}5 \cdot 10^{-7}$ and $BR(t \rightarrow cc) \sim 7\text{--}5 \cdot 10^{-9}$. In models with $Q = 1=3$ quark singlets, the respective branching ratios are much smaller since the breaking of the CKM unitarity is very constrained by experimental data⁸. The contributions arising from a sequential fourth generation b^0 to the FCNC top-quark decays have been also studied^{3;57}. However, the virtual effects induced by a b^0 heavy quark cannot enhance the respective branching ratios to within the LHC's reach: $BR(t \rightarrow cz) \sim 10^{-6}$, $BR(t \rightarrow cH) \sim 10^{-7}$ – 10^{-6} , $BR(t \rightarrow cg) \sim 10^{-7}$, $BR(t \rightarrow cc) \sim 10^{-8}$ ⁵⁷.

8. Three-body decays

The interest in FCNC three-body decays of the top quark relies in the phenomenon known as "higher order dominance", observed in b-physics, in which a higher order dominates over a lower order rate. Of course, the enhancements obtained in two-body FCNC decays might also appear in these decay modes in some extensions of the SM⁵⁸. According to the recent CDF/DO analysis based on the Tevatron RUN II data⁵⁹, the following three-body rare decays of the top quark may be allowed kinematically: $t \rightarrow bWZ$, $t \rightarrow cWZ$, $t \rightarrow cVW$ ($V = g; Z; \gamma$), $t \rightarrow c_i \bar{u}_j$, $t \rightarrow c_i u_j$. In particular, the decay $t \rightarrow czZ$ can only occur through finite-width effects in some range of the allowed parameter space of THDM-III⁶⁰.

In the SM, only the two decay modes $t \rightarrow bWZ$ and $t \rightarrow cWZ$ arise at the tree-level with branching ratios of order 10^{-12} – 10^{-14} ⁶¹. Since these decay channels occur near the kinematical threshold, the finite decay width of the W and Z bosons

induce sizeable enhancements on the respective branching ratios: $BR(t \rightarrow bWZ) \approx 2 \cdot 10^{-6}$ in the SM⁶², and $BR(t \rightarrow cW) \approx 10^{-3} \cdot 10^{-4}$ and $BR(t \rightarrow cZ) \approx 10^{-3}$ in the THDM-III⁶⁰.

The decay modes $t \rightarrow cV_jV_j$ have been estimated in the SM assuming that the respective decay rates are dominated by a Higgs-boson resonant diagram with a FCNC tcH vertex and the further two-body decay of the Higgs boson $H \rightarrow V_iV_j$ ²⁶. Using the SM values for the effective vertices tcH and HV_iV_j ^{4;5;19}, one gets the expected SM suppressed values: $BR(t \rightarrow cc)$, $BR(t \rightarrow cZ) \approx 10^{-15} \cdot 10^{-16}$ and $BR(t \rightarrow cgg) \approx 10^{-14} \cdot 10^{-15}$ ²⁶. In the latter case, a complete one-loop calculation in the SM gives $BR(t \rightarrow cgg) = 1.02 \cdot 10^{-9}$, two orders of magnitude higher than the two-body decay rate $BR(t \rightarrow cg) = 5.73 \cdot 10^{-12}$ ⁶³.

These decay modes have been studied also in the framework of the THDM-III within the same Higgs-boson resonant exchange approximation^{26;64}. In this case the enhancements obtained are sizeable due to the combined effect of the tree-level tcH coupling and the resonance of the intermediate Higgs boson: $BR(t \rightarrow cc)$, $BR(t \rightarrow cZ) \approx 10^{-4} \cdot 10^{-5}$ and $BR(t \rightarrow cW)$; $BR(t \rightarrow cgg) \approx 10^{-4}$ ²⁶ (Fig. 2). In the latter case, a complete one-loop calculation in the MSSM produces $BR(t \rightarrow cgg) \approx 10^{-7} \cdot 10^{-9}$, for reasonable values of the MSSM parameters, and $BR(t \rightarrow cgg)$; $BR(t \rightarrow cg) \approx 10^{-5}$ if the SUSY FCNC couplings are allowed to be large⁶⁵.

Models with additional Higgs triplets can include a tree-level vertex HWZ , the decay mode $t \rightarrow bWZ$ may then proceed by an intermediate charged Higgs boson, and the same resonance effect may induce a spectacular enhancement $BR(t \rightarrow bWZ) \approx 10^{-2}$ ⁵⁸. A similar situation happens with the radiative three body decay $t \rightarrow ch$ in the THDM-III, which also can proceed at the tree level with a large enhancement $BR(t \rightarrow ch) \approx 10^{-5}$ with respect to the SM prediction $BR(t \rightarrow ch)$.

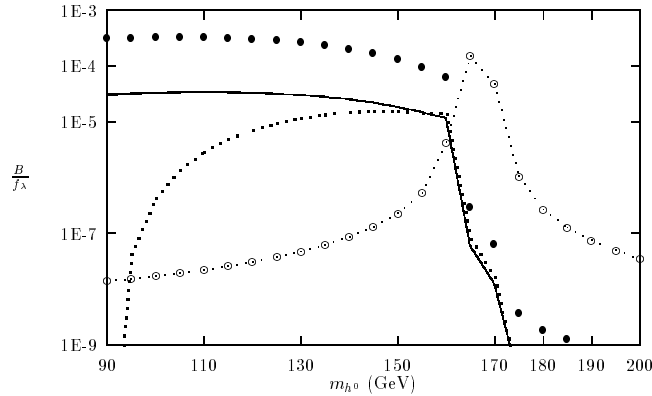


Fig. 2. Scaled branching ratios for $t \rightarrow cV_jV_j$ in the THDM-III: $t \rightarrow cc$ (solid line), $t \rightarrow cZ$ (points), $t \rightarrow cW$ (hollow circles), and $t \rightarrow cgg$ (full circles). The masses of the Higgs bosons H_1 ; A and H_2 were set to 750 GeV.

ch) $\sim 10^{-15}$ [66].

In TC2 models, the W^+W^- decay channel gets a substantial enhancement: $BR(t \rightarrow cW) \sim 10^{-3}$, but in the other $V_i V_j$ decay modes the enhancement is very small [67]. Finally, the three-body FCNC decay modes involving a lepton or a quark pair have been calculated in the THDM-III and TC2 models, but the respective branching ratios are out of the LHC's reach: $BR(t \rightarrow c\ell\ell)$, $BR(t \rightarrow c'q'q')$ $\sim 10^{-7} - 10^{-10}$ [63;68].

9. Constraints from loop observables

In the effective Lagrangian approach, the new physics effects induced by non-standard particles can be parameterized as coupling constants of effective operators which are constructed out of SM fields [69]. The SM Lagrangian is modified by the addition of a series of SM-gauge invariant operators with coefficients suppressed by inverse powers of Λ , the lowest new-physics scale. The largest contribution to top-quark FCNC comes from dimension-6 operators since dimension-5 operators violate lepton number [70]. After the spontaneous symmetry breakdown, the dimension-6 operators induce the most general effective Lagrangian given in Eq. (9), which describes the FCNC top-quark interactions with a light quark c or u and the gauge bosons $V = \gamma, g, Z$ and the SM Higgs boson H .

The possibility of extracting bounds on the effective vertices tcV and tcH from loop observables has been studied in different processes. Even though these bounds can not be considered model-independent constraints, they may be regarded as order of magnitude estimates which could be used in the search of new physics effects in the following generation of colliders [10].

The measurement of the inclusive branching ratio for the FCNC process $b \rightarrow c\ell\ell$

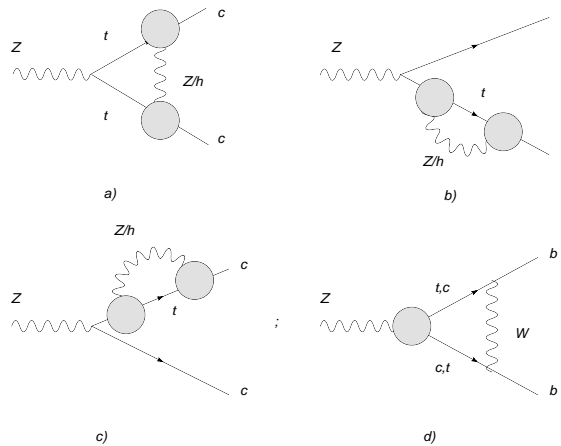


Fig. 3. Feynman diagrams for the one-loop contribution of the $tcZ=tcH$ vertices to the decay modes $Z \rightarrow bb, cc$.

14 F. Larios, R. Martinez and M. A. Perez

Eq. 71 has been used to put constraints on the tc ; tcg couplings [72;73]. These anomalous couplings modify the coefficients of the operators O_7 and O_8 of the effective Hamiltonian for the $b \rightarrow s$ transition. The known branching ratio for $t \rightarrow bW^+$ and the CLEO bound on $b \rightarrow s$ place the limits $|j_g| < 0.9$ and $|j_j| < 0.16$, which can be translated into the bounds $BR(t \rightarrow c) < 2.2 \cdot 10^{-3}$ and

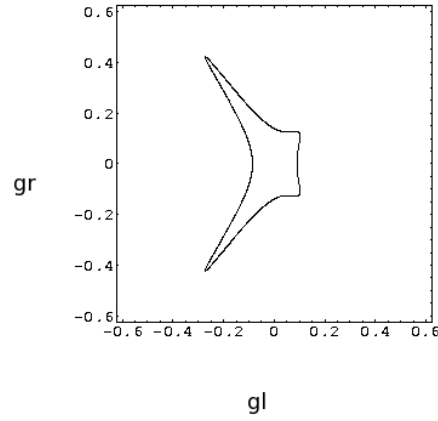


Fig. 4. A 95% C.L. plot on the bounds of the dimension-4 tcZ couplings obtained from the current values of the electroweak precision observables.

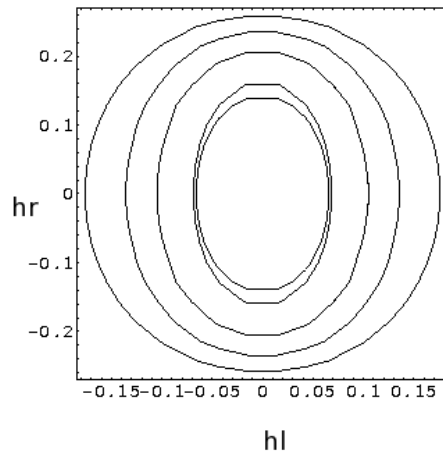


Fig. 5. A 95% C.L. plot on the bounds of the dimension-4 tcH couplings obtained from the current values of the electroweak precision observables. From the inner to the outer curves, the corresponding values for the Higgs boson mass are: 114, 130, 145, 150 and 160 GeV.

$BR(t \rightarrow c\gamma) < 3.4 \times 10^{-2}$ [72;73]. The tcZ couplings g_r and g_l given in Eq. (4) were bounded using several FCNC low-energy processes such as $K_L \rightarrow \pi^+ \pi^-$, $K_L \rightarrow K_S$ mass difference, $B^0 \rightarrow B^0$ mixing and $B \rightarrow \pi^+ \pi^-$, as well as the oblique parameters S and T : $g_r < 0.29$ and $g_l < 0.05$ [74]. Since the transition amplitude for the latter process is linear in the tcZ coupling, its decay rate is very sensitive to the FCNC

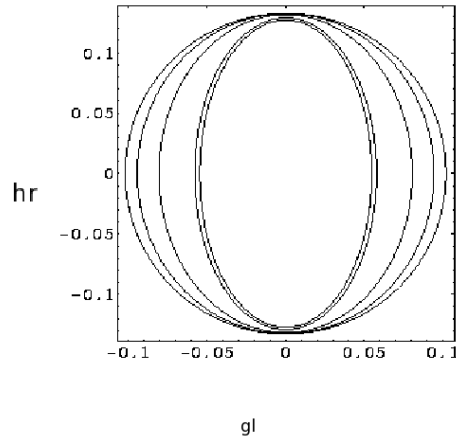


Fig. 6. A 95% CL constraint on the dimension four couplings h_r and g_l obtained from the interference of the contributions of the $tcH = tcZ$ effective vertices to the electroweak LEP precision observables. We fixed $g_r = h_l = 0.05$ and the values used for the Higgs mass are indicated in figure 5.

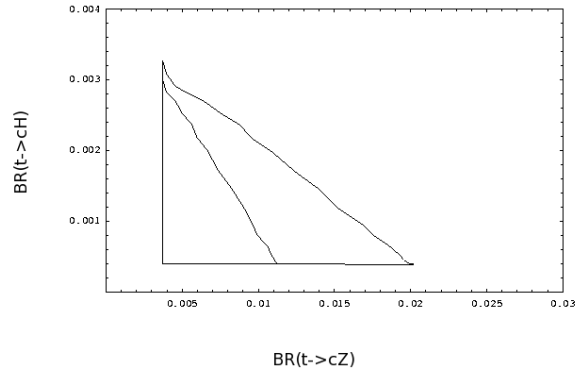


Fig. 7. A 95% CL constraint on the bounds expected for the branching ratios of the decays $t \rightarrow cH$ and $t \rightarrow cZ$ if use is made of the limits for the couplings $h_{r,l}$ and $g_{r,l}$ as given in Fig. 6. Two allowed regions are shown for $m_H = 114$ and 145 GeV: inner and outer triangles respectively.

tcZ coupling and produced a stringent limit, $|g_1| < 0.05$ ⁷⁴.

The FCNC couplings tcZ and tcH have also been constrained by using the electroweak precision observables R_Z, R_C, R_b, R_1, A_C and the S/T oblique parameters⁷⁵. The one-loop correction of these couplings to the decay modes $Z \rightarrow cc$ and $Z \rightarrow bb$ are shown in Fig. 3. Even though these vertices enter in the Feynman diagrams 3(b)–(d) as a second order perturbation, the known limits on the above precision observables¹ impose significant constraints on the tcH and tcZ couplings⁷⁵.

Figures 4 and 5 show the 95% C.L. limits on the $g_1=g_r$ and $h_1=h_r$ FCNC top quark vertices and for several values of the intermediate-mass Higgs boson. These limits can be translated into the following bounds for the respective branching ratios: $BR(t \rightarrow cZ) < 1.6 \cdot 10^{-2}$ and $BR(t \rightarrow cH) < 0.9 \cdot 29 \cdot 10^{-4}$ for $116 \text{ GeV} < m_H < 170 \text{ GeV}$ ⁷⁵.

In particular, the limit on $BR(t \rightarrow cZ)$ is similar to the bound recently reported by the DELPHI collaboration⁷⁶. On the other hand, the contribution of the dimension-5 terms shown in Eq.(4) to the Feynman diagrams shown in Fig. 3 are suppressed by a factor of order $(m_Z/m_t)^4$ with respect to the corrections induced by the dimension-4 terms tcZ and tcH . This is the reason why the $BR(t \rightarrow c)$ does not acquire any significant constraints from the above LEP precision observables⁷⁵. The interference of the tcH and tcZ contributions to the rate $Z \rightarrow bb$ does not improve the above limits (Figs. 6 and 7).

10. Summary and outlook

The FCNC decays of the top quark are very sensitive to physics beyond the SM. Some extensions of the SM predict spectacular enhancements on the FCNC branching ratios which are within the reach of the LHC and the ILC. Searches for FCNC top-quark effects in these colliders may thus constitute one of the best way to look for physics beyond the SM: the experimental feasibility of detecting such effects in top quark production and decays seems to be better than the situation expected in the FCNC effects of the Z gauge boson⁷⁷ and the Higgs boson⁷⁸ (or even in the case of the expected CP violating effects in top quark physics⁷⁹).

In Table 1 we summarize the predictions that are potentially visible at the LHC and ILC colliders for the different models surveyed in the present review. As we can appreciate, almost all models include testable predictions for the FCNC channels which will be accessible in these colliders. In this respect, even in the optimistic situation of a positive detection of a FCNC decay of the top quark, there would remain still the question to clear up the nature of the virtual effects involved in the enhancement of the respective FCNC decay. On the other hand, if no new physics effect is ever found in this search, an improvement on the experimental bounds of FCNC top quark decays will provide a critical test of the validity of the SM at the loop level.

Table 1. Summary of the predictions that are potentially visible at the LHC and ILC for BR-FCNC top-quark decay modes. References to specific results are included in the text. The column for the effective Lagrangian approach (ELA) includes the respective bounds obtained for these decay modes from low-energy precision measurements.

Decay	THDM II	THDM III	MSSM	\overline{R} -MSSM	TC2	L-R	LR-SUSY	Extra q	ELA
$t! c$	10^{-7}	10^{-7}	10^{-6}	10^{-5}	10^{-7}		10^{-6}	10^{-8}	10^{-3}
$t! cZ$	10^{-8}	10^{-6}	10^{-6}	10^{-4}	10^{-5}		10^{-4}	10^{-4}	10^{-2}
$t! cg$	10^{-5}	10^{-4}	10^{-4}	10^{-3}	10^{-5}		10^{-5}	10^{-7}	10^{-2}
$t! cH$	10^{-4}	10^{-3}		10^{-5}		10^{-4}		10^{-5}	10^{-3}
$t! cW$		10^{-3}			10^{-3}				
$t! cZZ$		10^{-3}							
$t! c$		10^{-4}							
$t! cZ$		10^{-4}							
$t! cgg$		10^{-4}	10^{-5}						
$t! cHg$		10^{-5}							

Acknowledgments

We thank Conacyt (Mexico) and Colciencias (Colombia) for support.

References

1. S. Eidelman et al, Particle Data Group Phys. Lett. B 592, 1 (2004).
2. S.L. Glashow, J. Iliopoulos, L. Maiani, Phys. Rev. D 2, 1285 (1970).
3. J.L. Diaz-Cruz, R. Martinez, M.A. Perez, A. Rosado, Phys. Rev. D 41, 891 (1990).
4. G. Eilam, J.L. Hewett, A. Soni, Phys. Rev. D 44, 1473 (1991); Erratum *ibid.* D 59, 039901 (1999).
5. B. Mele, S. Petrarca, A. Soddu, Phys. Lett. B 435, 401 (1998); H. Frisch, Phys. Lett. B 224, 179 (1989).
6. S.L. Glashow and S. Weinberg, Phys. Rev. D 15, 1958 (1977).
7. A. Cordero-Cid, M.A. Perez, J.J. Toscano and G. Tavares-Velasco, Phys. Rev. D 70, 074003 (2004).
8. Aguilar-Saavedra, Acta Phys. Pol. B 35, 2695 (2004); Phys. Rev. D 67, 035003 (2003); *ibid.* D 69, 099901 (2004); J.A. Aguilar-Saavedra and B.M. Nobre, Phys. Lett. B 553, 251 (2003); J.A. Aguilar-Saavedra and G.C. Branco, Phys. Lett. B 495, 347 (2000); J.A. Aguilar-Saavedra, Phys. Lett. B 502, 115 (2001).
9. T. Abe et al, Linear Collider Physics Resource Book for Snowmass 2001 - Part 3., hep-ex/0106057.
10. W. Wagner, Rept. Prog. Phys. 68, 2409 (2005); A. Juste et al, Report of the 2005 Snowmass Top/QCD Working Group, hep-ph/0601112; J.M. Yang, Ann. Phys. (N.Y.) 316, 529 (2005); D. Chakraborty, J. Knigsgberg, D. Rainwater, Ann. Rev. Nucl. Part. Sci. 53, 301 (2003); M. Beneke et al, Report of the 1999 CERN Workshop on SM physics (and more) at the LHC, Geneva, hep-ph/0003033.
11. S. Bachi et al. (D0 Collaboration), Phys. Rev. Lett. 74, 2632 (1995).
12. F. Abe et al. (CDF Collaboration), Phys. Rev. Lett. 74, 2626 (1995).
13. W. Hollik et al, Nucl. Phys. B 551, 3 (1999); Erratum *ibid.* B 557, 407 (1999).
14. E.M. alkawi and C.-P. Yuan, Phys. Rev. D 50, 4462 (1994); *ibid.* D 52, 472 (1995); F. Larios, E.M. alkawi and C.-P. Yuan, hep-ph/9704288.
15. F. Larios and C.-P. Yuan, Phys. Rev. D 55, 7218 (1997); O.J.P. Eboli, M.C. Gonzalez-Garcia and S.F. Novaes, Phys. Lett. B 415, 75 (1997).

18 F. Larios, R. Martinez and M. A. Perez

16. F. Larios, M. A. Perez and C.-P. Yuan, *Phys. Lett. B* 457, 334 (1999).
17. U. Baur et al., *Phys. Rev. D* 71, 054013 (2005); U. Baur, [hep-ph/0508151](#).
18. T. Han and J.L. Hewett, *Phys. Rev. D* 60, 074015 (1999).
19. J.F. Gunion et al., *The Higgs Hunter's Guide* (Addison Wesley, Reading, MA, (1990); SCIPP-89/13, [hep-ph/9302272](#)).
20. T.P. Cheng and M. Sher, *Phys. Rev. D* 35, 3484 (1987); M. Sher and Y. Yuan, *Phys. Rev. D* 44, 1461 (1991); J.L. Diaz-Cruz and G. Lopez-Castro, *Phys. Lett. B* 301, 405 (1993).
21. A. Antaramian, L.J. Hall and A. Rasin, *Phys. Rev. Lett.* 69, 1871 (1992); L.J. Hall and S. Weinberg, *Phys. Rev. D* 48, 979 (1993); M.J. Savage, *Phys. Lett. B* 266, 135 (1991); M. Luke and M.J. Savage, *Phys. Lett. B* 307, 387 (1993).
22. D. Atwood, L. Reina and A. Soni, *Phys. Rev. D* 53, 1199 (1996); *Phys. Rev. Lett.* 75, 3800 (1975); *Phys. Rev. D* 55, 3156 (1997); B. Grzadowski, J.F. Gunion and P. Kravczyk, *Phys. Lett. B* 268, 106 (1991).
23. A. Arribas, *Phys. Rev. D* 72, 075016 (2005).
24. S. Bejar, J. Guasch, J. Sola, *Nucl. Phys. B* 675, 270 (2003).
25. E.O. Ilhan, *Phys. Rev. D* 65, 075017 (2002); E.O. Ilhan and I. Turan, *Phys. Rev. D* 67, 015004 (2003); W.S. Hou, *Phys. Lett. B* 296, 179 (1992).
26. J.L. Diaz-Cruz, M. A. Perez, G. Tavares-Velasco and J.J. Toscano, *Phys. Rev. D* 60, 115014 (1999); R.A. Diaz, R. Martinez and J. Alexis Rodriguez, [hep-ph/0103307](#).
27. D.J.H. Chung et al., *Phys. Rept.* 407, 1 (2005).
28. C.S. Li, R.J. Oakes and J.M. Yang, *Phys. Rev. D* 49, 293 (1994); Erratum *ibid.* D 56, 3156 (1997).
29. G. Couture, C. Hamzaoui and H. Konig, *Phys. Rev. D* 52, 1713 (1995); G. Couture, M. Frank and H. Konig, *Phys. Rev. D* 56, 4213 (1997).
30. J.L. Lopez, D.V. Nanopoulos and R. Rangarajan, *Phys. Rev. D* 56, 3100 (1997).
31. G.M. de Divitiis, R. Petronzio and L. Silvestrini, *Nucl. Phys. B* 504, 45 (1997).
32. J. Guasch and J. Sola, *Nucl. Phys. B* 562, 3 (1999); S. Bejar, J. Guasch and J. Sola, [hep-ph/0101294](#).
33. D. Delapine and S. Khalil, *Phys. Lett. B* 599, 62 (2004).
34. M. Misiak, S. Pokorski and J. Rosiek, *Adv. Ser. Direct. High Energy Phys.* 15, 798 (1997); also in [hep-ph/9703442](#).
35. J.J. Liu, C.S. Li, L.L. Yang and L.G. Jin, *Phys. Lett. B* 599, 92 (2004).
36. J.M. Yang, B.-L. Young and X. Zhang, *Phys. Rev. D* 58, 055001 (1998).
37. J.M. Yang and C.S. Li, *Phys. Rev. D* 49, 3412 (1994).
38. J.L. Diaz-Cruz, H.-J. He and C.-P. Yuan, *Phys. Lett. B* 530, 179 (2002).
39. J. Cao, G. Eilam, K.-I. Hikasa and J.M. Yang, [hep-ph/0604163](#).
40. G. Eilam et al., *Phys. Lett. B* 510, 227 (2001).
41. N. Escudero, C. Mueoz and A.M. Teixeira, *Phys. Rev. D* 73, 055015 (2006).
42. S. Weinberg, *Phys. Rev. D* 13, 974 (1976); L. Susskind, *Phys. Rev. D* 20, 2619 (1979).
43. S. Dimopoulos and S. Susskind, *Nucl. Phys. B* 155, 237 (1979); E. Eichten and L. Kane, *Phys. Lett. B* 90, 125 (1980).
44. C.T. Hill, *Phys. Lett. B* 345, 283 (1995); K. Lane, *Phys. Lett. B* 433, 96 (1998); G. Cvetic, *Rev. Mod. Phys.* 71, 513 (1999).
45. M.B. Popovic and E.H. Simmons, *Phys. Rev. D* 58, 095007 (1998).
46. B.A. Dobrescu and C.T. Hill, *Phys. Rev. Lett.* 81, 2634 (1998); R.S. Chivukula, B.A. Dobrescu, H. Georgi and C.T. Hill, *Phys. Rev. D* 59, 075003 (1999); H.J. He and C.T. Hill, *Phys. Rev. D* 65, 055006 (2002).
47. H.J. He, T.M.P. Tait and C.P. Yuan, *Phys. Rev. D* 62, 011702 (2000).
48. C.T. Hill and E.H. Simmons, *Phys. Rep.* 381, 235 (2003); Erratum *ibid.* 390, 553

- (2004).
49. X. Wang et al, Phys. Rev. D 50, 5781 (1994); J. Phys. G 20, 291 (1994); G. Lu et al, J. Phys. G 22, 305 (1996); Phys. Rev. D 57, 1755 (1998).
 50. G. Lu et al, Phys. Rev. D 68, 015002 (2003); C. X. Yue et al, Phys. Rev. D 64, 095004 (2001); G. Burdman, Phys. Rev. Lett. 83, 2888 (1999).
 51. F. Pisano and V. Plitzke, Phys. Rev. D 46, 410 (1992); P. H. Frampton, Phys. Rev. Lett. 69, 2889 (1992).
 52. C. X. Yue, H. J. Zong and L. J. Liu, Mod. Phys. Lett. A 18, 2187 (2003); A. Cordero-Cid, G. Tavares-Velasco and J. J. Toscano, Phys. Rev. D 72, 057701 (2005).
 53. R. N. Mohapatra, *Unification and Supersymmetry*, (Springer, New York, 2003), and references therein.
 54. A. Davidson and K. C. Wali, Phys. Rev. Lett. 59, 393 (1987); S. Rajpoot Phys. Lett. B 191, 122 (1987); K. Kiers et al, Phys. Rev. D 66, 095002 (2002).
 55. R. Gaitan, O. G. Miranda and L. G. Cabral-Rosetti, Phys. Rev. D 72, 034018 (2005); hep-ph/0604170.
 56. M. Frank and I. Turan, Phys. Rev. D 72, 035008 (2005).
 57. A. Arribas and W. S. Hou, hep-ph/0602035.
 58. J. L. Diaz-Cruz and D. A. Lopez, Phys. Rev. D 61, 051701 (2000).
 59. CDF/D0 Collaborations, <http://www-cdf.fnal.gov/physics/new/top/top.html>.
 60. S. Bar-Shalom et al, Phys. Rev. D 72, 055018 (2005).
 61. E. Jenkins, Phys. Rev. D 56, 458 (1997); D. Atwood and M. Sher, Phys. Lett. B 411, 306 (1997); R. Decker, M. Nowakowski and A. Pilaftsis, Z. Phys. C 57, 339 (1993).
 62. G. Altarelli, L. Conti, V. Lubicz, Phys. Lett. B 502, 125 (2001).
 63. G. Eilam, M. Frank and I. Turan, hep-ph/0601151.
 64. S. Bar-Shalom et al, Phys. Rev. Lett. 79, 1217 (1997); Phys. Rev. D 57, 2957 (1998); C. S. Li, B. Q. Hu and J. M. Yang, Phys. Rev. D 51, 4971 (1995); *ibid.* D 53, 5325 (1996).
 65. G. Eilam, M. Frank and I. Turan, hep-ph/0601253.
 66. A. Cordero-Cid et al, J. Phys. G 32, 529 (2006).
 67. C. X. Yue et al, Phys. Lett. B 508, 290 (2001).
 68. C. X. Yue, L. Wang and D. Yu, Phys. Rev. D 70, 054011 (2004).
 69. J. L. Diaz-Cruz, M. A. Perez and J. J. Toscano, Phys. Lett. B 398, 347 (1997); B. Grzadkowski et al, Nucl. Phys. B 689, 108 (2004); Phys. Lett. B 593, 189 (2004).
 70. W. Buchmuller and D. Wyler, Nucl. Phys. B 268, 621 (1986).
 71. M. Alam et al, CLEO Collaboration, Phys. Rev. Lett. 74, 2885 (1995).
 72. R. Martinelli, M. A. Perez and J. J. Toscano, Phys. Lett. B 340, 91 (1994); J. Feliciano et al, Rev. Mex. Fis. 42, 571 (1996).
 73. T. Han et al, Phys. Rev. D 55, 7241 (1997); G. Burdman, M. C. Gonzalez Garcia and S. F. Novaes, Phys. Rev. D 61, 114016 (2000).
 74. T. Han, R. D. Peccei and X. Zhang, Nucl. Phys. B 454, 527 (1995); R. D. Peccei, S. Peris and X. Zhang, Nucl. Phys. B 349, 305 (1991); R. D. Peccei and X. Zhang, Nucl. Phys. B 337, 269 (1990).
 75. F. Larios, M. A. Perez and R. Martinelli, Phys. Rev. D 72, 057504 (2005); R. Diaz, R. Martinez and C. E. Sandoval, Eur. Phys. J. C (to appear).
 76. I. Abdalla et al, DELPHI Collaboration, Phys. Lett. B 590, 21 (2004).
 77. M. A. Perez, G. Tavares-Velasco and J. J. Toscano, Int. J. Mod. Phys. A 19, 159 (2004).
 78. J. L. Diaz-Cruz and J. J. Toscano, Phys. Rev. D 66, 116005 (2002); D. Black et al, Phys. Rev. D 66, 053002.
 79. D. Atwood et al, Phys. Rept. 347, 1 (2001).